Universal Recovery of the Energy-Level Degeneracy of Bright Excitons in InGaAs Quantum Dots without a Structure Symmetry

R. Trotta,[1,2,*] E. Zallo,[1] C. Ortix,[3] P. Atkinson,[1,4] J. D. Plumhof,[1] J. van den Brink,[3] A. Rastelli,[1,2,†] and O. G. Schmidt[1]

[1]*Institute for Integrative Nanosciences, IFW Dresden, Helmholtzstrasse 20, D-01069 Dresden, Germany*
[2]*Institute of Semiconductor and Solid State Physics, Johannes Kepler University Linz, Altenbergerstrasse 69, A-4040 Linz, Austria*
[3]*Institute for Theoretical Solid State Physics, IFW Dresden, Helmholtzstrasse 20, D-01069 Dresden, Germany*
[4]*Institut des NanoSciences des Paris, UPMC CNRS UMR 7588, 4 Place Jussieu Boite courier 840, Paris 75252 Cedex 05, France*

(Received 7 June 2012; published 1 October 2012)

The lack of structural symmetry which usually characterizes semiconductor quantum dots lifts the energetic degeneracy of the bright excitonic states and hampers severely their use as high-fidelity sources of entangled photons. We demonstrate experimentally and theoretically that it is always possible to restore the excitonic degeneracy by the simultaneous application of large strain and electric fields. This is achieved by using one external perturbation to align the polarization of the exciton emission along the axis of the second perturbation, which then erases completely the energy splitting of the states. This result, which holds for any quantum dot structure, highlights the potential of combining complementary external fields to create artificial atoms meeting the stringent requirements posed by scalable semiconductor-based quantum technology.

DOI: 10.1103/PhysRevLett.109.147401 PACS numbers: 78.67.Hc, 71.70.Gm, 81.07.Ta, 85.35.Be

Semiconductor quantum dots (QDs) are nanostructures made of several thousands of atoms which can self-assemble during epitaxial growth. In spite of the remarkable progress in QD fabrication [1,2], unavoidable fluctuations in the exact number of atoms, their arrangement in the host matrix, and intermixing with the substrate and the cap material make each QD unique. As a result, the possibility to grow semiconductor QDs showing specific properties of symmetry is a mere theoretical construct [3,4]. This represents an enormous obstacle towards the exploitation of QDs in quantum technologies, where the precise control over the QD emission properties is a fundamental requirement [5]. In particular, the absence of structural symmetry usually occurring in real QDs induces a coherent coupling of the two bright excitonic states [6–10] which leads to an energetic separation between them—the so-called fine structure splitting (FSS, s). When the FSS is larger than the radiative line width of the transitions (of the order of 1 μeV), the fidelity of the entangled photon pairs emitted during the decay biexciton-exciton-ground state is strongly reduced [11–14]. For more than a decade researchers have struggled to find a reproducible way to suppress the FSS and, to date, some quantum optics experiments are still carried out with the rare QDs showing sufficiently small FSS [15,16]. The origin and magnitude of the FSS are mainly determined by the QD morphology, piezoelectricity, alloying, and the symmetry of the underlying lattice [17–20]. Recently, the possibility to use single external perturbations such as electric [6,21,22], magnetic [14], and strain fields [7,23,24] to erase the FSS has been explored. Theoretical [25,26] and experimental [6,7] results have demonstrated that there is a lower bound of the FSS (usually larger than 1 μeV) caused by the coherent coupling of the two bright exciton states. On the other hand, there are a few works reporting values of the FSS close to zero [14,27], but it remains unclear whether a strictly zero FSS can be universally achieved, especially considering that it is commonly believed that the excitonic degeneracy cannot be restored in QDs with low structural symmetry [25,28]. In this Letter, we demonstrate that the coupling between the bright excitons can be reversibly controlled and erased by the simultaneous application of large strain and electric fields, thereby showing that it is always possible to drive the excitons confined in arbitrary QDs towards a universal level crossing.

The device employed in this work is shown schematically in Fig. 1(a). Thin n-i-p nanomembranes containing QDs are integrated onto $[Pb(Mg_{1/3}Nb_{2/3})O_3]_{0.72}$-$[PbTiO_3]_{0.28}$ (PMN-PT) piezoelectric actuators by gold-thermocompression bonding, as described elsewhere [29]. The quantum emitters (InGaAs QDs) were grown on GaAs (001) by solid source molecular beam epitaxy and were placed in the center of a 10 nm-thick $GaAs/Al_{0.4}Ga_{0.6}As$ quantum well. As compared to structures without well, this layer sequence reduces carrier ionization at high electric fields across the diode (F_d) and allows the QD emission lines to be shifted over a broad spectral range by applying a reverse bias (V_d) to the nanomembranes [6]. Simultaneously, a voltage V_p (electric field F_p) applied to the PMN-PT induces in-plane (compressive or tensile) biaxial strains in the QD layer, which allow the energy of the QD emission lines to be controlled in a well-defined manner [29–31]. The voltage applied to the PMN-PT and diode usually vary in the ranges $-350\ \text{V} < V_p < 900\ \text{V}$ and $-1.9\ \text{V} < V_d < 2\ \text{V}$, respectively. The in-plane strain transferred to the GaAs nanomembranes varies by about

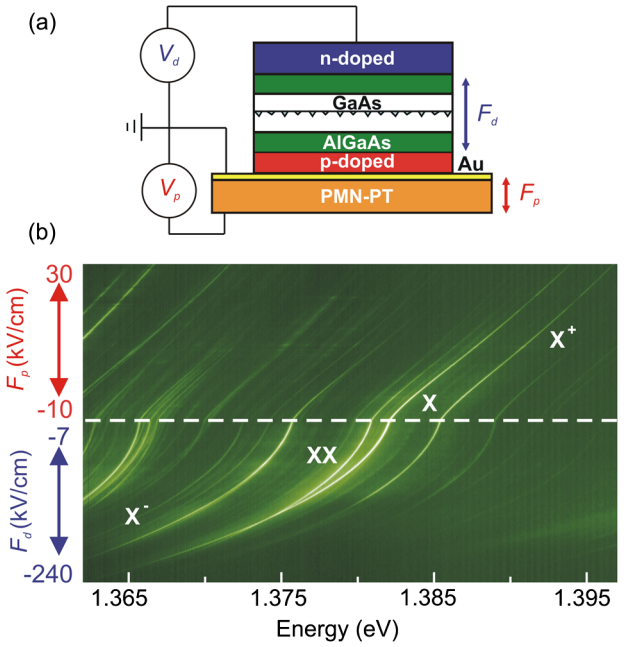

FIG. 1 (color online). (a) Sketch of the device. An *n-i-p* nanomembrane featuring the so-called "giant Stark effect" [6] is integrated on top of a piezoelectric actuator (PMN-PT) allowing the *in situ* application of anisotropic biaxial strains [in the (001) plane of the GaAs nanomembranes] by tuning the voltage (electric field) V_p (F_p). Independently, a voltage applied to the nanomembrane (V_d) allows the electric field (F_d) along the [001] direction to be controlled. (b), Color-coded microphotoluminescence (μ-PL) map of a single QD as a function of F_p and F_d. The two fields were varied one after the other, i.e., $F_p = -10$ kV/cm when F_d is ramped up (bottom), whereas $F_d = -7$ kV/cm when F_p is ramped up (top). The abscissa indicates the energy of the emitted photons. The ordinate indicates the value of F_p and F_d used in the experiment. The exciton (X), biexciton (XX), and charged exciton (X^+ and X^-) transitions from the same QD were identified by polarization-resolved μ-PL spectroscopy.

0.3%–0.4% when V_p is swept through the whole tuning range [29]. It is also important to note that the biaxial strain transferred to the QDs via the PMN-PT is anisotropic in the plane, as found in very similar devices [30]. This anisotropy, which was not considered in Ref. [31], is of crucial importance for this work.

Standard low-temperature (4–10 K) micro photoluminesce spectroscopy was used for the optical characterization of the device, which was excited with a 850 nm continuous-wave laser. Polarization-resolved measurements were performed by inserting in the optical path a linear-polarization-analyzer composed of a rotating half-lambda wave plate and a linear polarizer, whose transmission axis was set along the [110] crystal direction of the nanomembrane with 10° accuracy. The FSS and the polarization angle of the excitonic emission were evaluated using the same procedure reported in Ref. [6], which ensures submicroelectronvolt resolution; see the Supplemental Material [32].

The device shown in Fig. 1(a) combines the most powerful "tuning knobs" available to date (electric and strain fields) and allows the QD emission properties to be engineered on demand. This is, for example, demonstrated in Fig. 1(b), where the two knobs are used for tuning all the QD emission lines across a spectral range larger than 30 meV. Furthermore, control over the binding energies of biexciton (XX) and charged excitons (X^+ and X^-) is also demonstrated in Fig. 1(b), as reported previously with either electric fields or strain [6,31]. We now show that the possibility to apply *simultaneously* two *independent* external fields allows a fundamental problem plaguing QDs (the presence of a coherent coupling of excitons) to be solved.

The coupling between the bright excitonic states can be highlighted by sweeping their energetic levels one across the other [6,7,25]. This is shown schematically in Fig. 2(a), where the two excitonic states (X_1 and X_2) undergo an avoided crossing as the magnitude of an external field is varied. The minimum s value (Δ) is a measure of the coupling strength and θ is the polarization angle of the low energy transition with respect to the [110] crystal direction. Figures 2(b) and 2(c) show the experimental behavior of s and θ for a QD as a function of F_p (F_d) with $V_d = 0$ ($V_p = 0$). It is evident that the effects produced by the two fields on s and θ are *qualitatively* similar [they follow the anticrossing pattern sketched in Fig. 2(a)], but *quantitatively* distinct. In particular, the values of Δ are very different, implying that the coupling is not only an intrinsic property of the QD under consideration, but it is influenced by the strength and symmetry of the external perturbations.

Figure 3(a) shows the behavior of the FSS for another QD as a function of F_d for different values of F_p. For tensile strain ($F_p < 0$), the value of Δ increases up to a maximum observed value of $\Delta_{\max} \sim 25$ μeV, while under compressive strain ($F_p > 0$) Δ first decreases to a minimum value ($\Delta_{\min}$) and then increases again. As seen more clearly in Fig. 3(b), where the FSS is plotted against the exciton energy (E_x) in the region of small FSS, the value of $\Delta_{\min}$ is comparable with the experimental spectral resolution (~ 0.5 μeV). This figure also highlights that FSS smaller than 1 μeV can be obtained for different exciton emission energies (~ 1 meV in this specific case). This could be of high potential interest for entanglement swapping between independent and remote QD-based quantum bits [5]. Similar results were obtained in 4 other QDs chosen randomly in our device [see Fig. 3(c)]. This evidence, along with the fact that even the FSS of a QD showing $\Delta_{\max}$ as large as 40 μeV can be tuned to values below 0.5 μeV, strongly suggests that electro-elastic fields enable us to "erase" the FSS of most of the QDs in our sample. Since the values of Δ typically observed in experiments performed with InGaAs QDs rarely exceed 40 μeV [6,7], we expect our result to be generally relevant.

Additional information can be found studying the behavior of θ [see Fig. 4(a)] for the same QD reported in

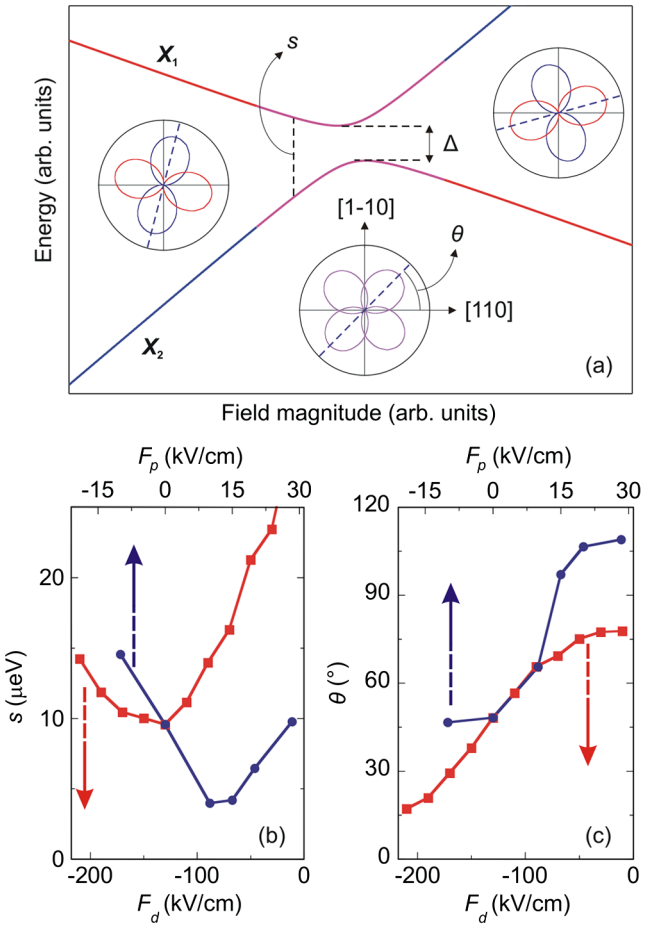

FIG. 2 (color online). (a) Sketch of the energetic levels of the two bright excitonic states (X_1 and X_2) when they are swept across each other under the influence of a generic external field. The colors highlight the character of the states. The energetic distance between the two levels is the FSS (s), and Δ is a measure of the coupling strength between the states. The insets show a sketch of the angular distribution in the (001) plane of the light emitted by the two exciton transitions. The two components are assumed to have the same oscillator strength and to be oriented at 90° with respect to each other. The angle θ represents the polarization angle of the lowest energy transition with respect to the [110] crystal direction. (b) Measured behavior (symbols connected by lines) of the FSS for a QD as a function of F_p and F_d, top and bottom axis, respectively. (c) Behavior of the polarization angle θ (symbols connected by lines) for the same QD of Fig. 2(b) as a function of F_p and F_d, top and bottom axis, respectively. In (b) and (c), the data as a function of F_p (F_d) are obtained with $V_d = 0$ ($V_p = 0$).

Fig. 3(a). When F_p is increased, the θ curve shows sharper variations with F_d and, after the critical point where $\Delta = \Delta_{\min}$, the direction of rotation is inverted, from anticlockwise to clockwise. This change in the handedness of θ suggests that the $s = 0$ critical point has been crossed. Obviously, the finite spectral resolution of the experimental apparatus prevents $s = 0$ to be proved, but the fact that we observe systematically the same behavior in all the QDs we measured indicates the existence of a universal behavior of the FSS under the influence of strain and electric fields, despite the different properties of the quantum emitters. In order to check if $s = 0$ can be achieved, we now analyze the experimental observations theoretically.

The FSS originates from the breaking of the D_{2d} or C_{4v} symmetry occurring even in ideal QDs with C_{2v} symmetry [10]. Any additional disorder (we can safely assume that any realistic QD has only C_1 symmetry) implies that the polarization angle of the bright excitons further departs from the pure lens shaped ones [10,25,33]. Whether or how the FSS can be tuned to zero depends on the existence of external perturbations able to "universally" restore the level degeneracy, independent of the specific QD parameters. By considering the combined effect of a vertical electric field (F) applied along the [001] direction and anisotropic biaxial stresses [30] of magnitude $p = p_1 - p_2$, where p_1 and p_2 are the magnitudes of two perpendicular stresses applied along arbitrary directions in the (001) plane, the effective two-level Hamiltonian for the bright excitons takes the form [32]

$$H = [\eta + \alpha p + \beta F]\sigma_z + [k + \gamma p]\sigma_x,$$

where $\sigma_{z,x}$ are the usual Pauli matrices, and η and k account for the QD structural asymmetry. The parameters related to the external fields are α and γ (related to the elastic compliance constants renormalized by the valence band deformation potentials), and β (proportional to the difference of the exciton dipole moments). Diagonalization of the above Hamiltonian gives the following values of s and θ:

$$s = [(\eta + \alpha p + \beta F)^2 + (k + \gamma p)^2]^{1/2}, \quad (1)$$

$$\tan\theta_{\pm} = \frac{k + \gamma p}{\eta + \alpha p + \beta F \pm s}. \quad (2)$$

Equations (1) and (2) are used to fit the experimental data with the parameters of the QD fixed [32]. As shown in Figs. 3(a) and 4(a), an excellent agreement is found. Even more, the theory predicts $s = 0$ and, after this critical point, there is an inversion in the handedness of θ. Therefore, the change in handedness can be considered as the experimental signature of the crossing of the $s = 0$ critical point. Most importantly, it can be easily shown that Eq. (1) has *always* a minimum at zero when the magnitude of F and p take the values

$$p_{\text{critic}} = -\frac{k}{\gamma}, \qquad F_{\text{critic}} = \frac{\alpha k}{\gamma\beta} - \frac{\eta}{\beta}.$$

In other words, there are *always* values of F_p and F_d such that $s = 0$, regardless of the QD structure. It is obvious that in real experiments large enough tuning ranges are needed to access the values of p_{critic} and F_{critic} given above. This requirement appears to be satisfied by our device, which allows us to tune systematically all the QDs we measure to

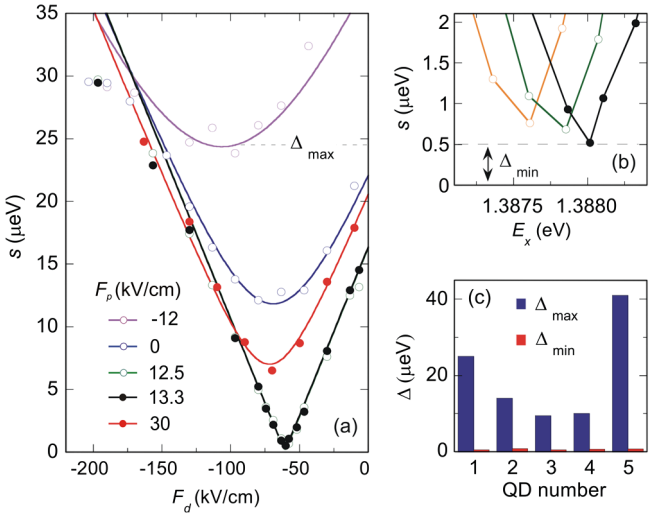

FIG. 3 (color online). (a), Behavior of the FSS as a function of F_d. The different curves correspond to different values of F_p. Empty (full) circles show the experimental data for F_p smaller (larger) than 13 kV/cm, which approximately corresponds to the critical strain condition for which the FSS reaches 0 as F_d is varied. The solid lines are fits to the experimental data obtained using Eqs. (1) and (2). Δ_{max} indicates the maximum value of Δ observed by combining both tuning knobs for this specific QD. (b) FSS as a function of the energy of the excitonic transition (E_x) in the region of small FSS (circles connected by lines). The colors correspond to the F_p values shown in Fig. 3(a). The data taken at $F_p = 12$ kV/cm, not displayed in Fig. 3(a) for clarity purposes, are also reported (orange points connected by lines). The value of the minimum Δ is denoted Δ_{min}. (c) Histogram of Δ_{max} and Δ_{min} for the different measured QDs.

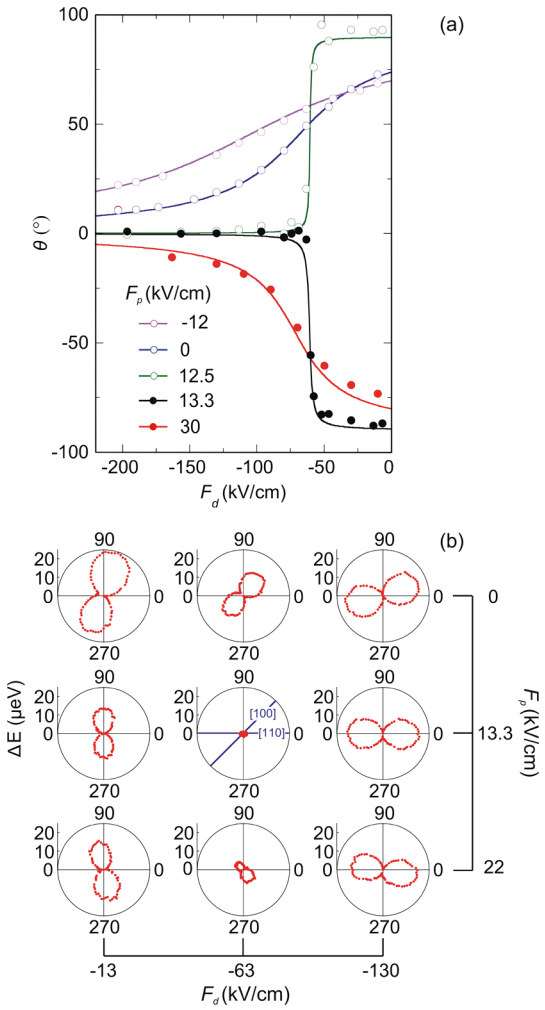

FIG. 4 (color online). (a), Behavior of the polarization angle (θ) as a function of F_d for the same QD whose FSS data are reported in Fig. 3(a). Different curves correspond to different values of F_p. The same symbols and colors of Fig. 3(a) for the different values of F_p have been used. The solid lines are fits to the experimental data obtained using equations (1) and (2). The direction of rotation of the eigenstates with F_d is inverted after crossing $s = 0$, which occurs for $F_p \sim 13$ kV/cm. (b) Dependence (in polar coordinates) of ΔE vs φ; see text. The length and the orientation of the petals give the value of the FSS and θ, respectively. Specific values of F_p and F_d around FSS ~ 0 have been used to construct this plot. Note that around the point where the FSS $= 0$ (central panel) the phase rotates in the whole tuning range (180°) under the effect of the two fields. In the central panel, the [110] and [100] crystal directions of the nanomembrane are also indicated.

$s = 0$. It is also important to observe that the remarkable agreement between all the experimental data and the simple theory developed in this work indicates that higher order terms in p and F can be neglected. The result is in line with those obtained with a single perturbing field [26], where a good agreement between this continuum theory and atomistic calculations is found.

Finally, by combining the theoretical analysis with the experimental data a clear and intuitive picture emerges. Figure 4(b) shows the dependence (in polar coordinates) of ΔE vs φ for specific values of F_p and F_d, where $\Delta E = |E(\varphi, F_p, F_d) - E_{min}(F_p, F_d)|$ and φ is the angle between the linear-polarization-analyzer and the [110] crystal direction. $E(\varphi, F_p, F_d)$ is half of the difference between the X and XX emission energies (see Ref. [6]) and $E_{min}(F_p, F_d)$ is the minimum value of $E(\varphi, F_p, F_d)$ averaged over 360° rotation of the wave plate. Therefore, the length and the orientation of the "petals" give the magnitude of the FSS and θ, respectively. It is clear that when the eigenstates are oriented along the [110] (close to the [100]) or the perpendicular direction, the application of F_d (F_p) leads to $s = 0$. Since electric and strain fields act as effective deformations along, respectively, the [110] and close to the [100] directions [32], this implies that the excitonic degeneracy can be restored if one external perturbation (e.g., F_d) is used to align the polarization axis of the exciton emission along the axes of the second perturbation (e.g., F_p), which is then able to compensate *completely* for the difference of the confining potentials of the two bright exciton eigenstates, i.e., is able to tune the FSS to zero.

This explains also why a lower bound of the FSS is usually observed with single external fields [6,7,25,26], where the probability to find a QD whose polarization axis is aligned along the axis of the tuning knob is extremely low. The above discussion highlights the crucial importance of having at hand *two independent* and *broad-range* "tuning knobs" for controlling *both* the FSS and the polarization direction of the exciton emission.

In conclusion, we have presented an all-electrically controlled device where the QD emission properties are engineered by large electro-elastic fields provided by diode-like nanomembranes integrated onto piezoelectric actuators. In particular, we have demonstrated that the simultaneous application of electric and elastic fields allow us to control and cancel the coherent coupling between the bright excitonic states—and hence the exciton fine structure splitting—in all the quantum dots we measure. The experimental observations are supported by a simple theoretical model which holds for every QD structure. The tedious search for QDs suitable for quantum optics experiments can therefore be avoided, and a deterministic implementation of high-fidelity sources of entangled photons into a scalable semiconductor-based quantum-information technology seems much more likely in the foreseeable future.

We thank E. Magerl, S. Kumar, A. Schliwa, and V. Fomin for fruitful discussion; B. Eichler, R. Engelhardt, and D. Grimm for technical support; and K. Dörr and A. Herklotz for help with the piezoelectric actuators. The work was supported financially by BMBF QuaHL-Rep (Contract No. 01BQ1032) and DFG FOR730.

Note added in proof.—Recently we became aware that Wang *et al.* [34] have theoretically suggested that the FSS can be also suppressed by combined stresses along the [110] and [010] directions.

*rinaldo.trotta@jku.at
†armando.rastelli@jku.at

[1] L. O. Mereni, V. Dimastrodonato, R. J. Young, and E. Pelucchi, Appl. Phys. Lett. **94**, 223121 (2009).
[2] *Lateral Alignment of Epitaxial Quantum Dots* edited by O. G. Schmidt (Springer, Berlin, 2007).
[3] A. Rastelli, M. Stoffel, A. Malachias, T. Merdzhanova, G. Katsaros, K. Kern, T. H. Metzger, and O. G. Schmidt, Nano Lett. **8**, 1404 (2008).
[4] M. Müller, A. Cerezo, G. D. W. Smith, L. Chang, and S. S. A. Gerstl, Appl. Phys. Lett. **92**, 233115 (2008).
[5] N. Gisin and R. Thew, Nature Photon. **1**, 165 (2007).
[6] A. J. Bennett, M. A. Pooley, R. M. Stevenson, M. B. Ward, R. B. Patel, A. Boyer de la Giroday, N. Sköld, I. Farrer, C. A. Nicoll, D. A. Ritchie, and A. J. Shields, Nature Phys. **6**, 947 (2010).
[7] J. D. Plumhof *et al.*, Phys. Rev. B **83**, 121302(R) (2011).
[8] M. Bayer *et al.*, Phys. Rev. B **65**, 195315 (2002).
[9] D. Gammon, E. S. Snow, B. V. Shanabrook, D. S. Katzer, and D. Park, Science **273**, 87 (1996).
[10] G. Bester, S. Nair, and A. Zunger, Phys. Rev. B **67**, 161306 (R) (2003).
[11] O. Benson, C. Santori, M. Pelton, and Y. Yamamoto, Phys. Rev. Lett. **84**, 2513 (2000).
[12] N. Akopian, N. H. Lindner, E. Poem, Y. Berlatzky, J. Avron, D. Gershoni, B. D. Gerardot, and P. M. Petroff, Phys. Rev. Lett. **96**, 130501 (2006).
[13] R. M. Stevenson, R. J. Young, P. Atkinson, K. Cooper, D. A. Ritchie, and A. J. Shields, Nature (London) **439**, 179 (2006).
[14] A. J. Hudson, R. M. Stevenson, A. J. Bennett, R. J. Young, C. A. Nicoll, P. Atkinson, K. Cooper, D. A. Ritchie, and A. J. Shields, Phys. Rev. Lett. **99**, 266802 (2007).
[15] C. L. Salter, R. M. Stevenson, I. Farrer, C. A. Nicoll, D. A. Ritchie, and A. J. Shields, Nature (London) **465**, 594 (2010).
[16] A. Dousse, J. Suffczyński, A. Beveratos, O. Krebs, A. Lemaître, I. Sagnes, J. Bloch, P. Voisin, and P. Senellart, Nature (London) **466**, 217 (2010).
[17] M. Abbarchi, C. A. Mastrandrea, T. Kuroda, T. Mano, K. Sakoda, N. Koguchi, S. Sanguinetti, A. Vinattieri, and M. Gurioli, Phys. Rev. B **78**, 125321 (2008).
[18] R. Seguin, A. Schliwa, S. Rodt, K. Pötschke, U. W. Pohl, and D. Bimberg, Phys. Rev. Lett. **95**, 257402 (2005).
[19] W. Langbein, P. Borri, U. Woggon, V. Stavarache, D. Reuter, and A. D. Wieck, Phys. Rev. B **69**, 161301(R) (2004).
[20] A. Schliwa, M. Winkelnkemper, and D. Bimberg, Phys. Rev. B **76**, 205324 (2007).
[21] B. D. Gerardot *et al.*, Appl. Phys. Lett. **90**, 041101 (2007).
[22] M. M. Vogel, S. M. Ulrich, R. Hafenbrak, P. Michler, L. Wang, A. Rastelli, and O. G. Schmidt, Appl. Phys. Lett. **91**, 051904 (2007).
[23] S. Seidl, M. Kroner, A. Högele, K. Karrai1, R. J. Warburton, A. Badolato, and P. M. Petroff, Appl. Phys. Lett. **88**, 203113 (2006).
[24] C. E. Kuklewicz, R. N. E. Malein, P. M. Petroff, and B. D. Gerardot, Nano Lett. **12**, 3761 (2012).
[25] R. Singh and G. Bester, Phys. Rev. Lett. **104**, 196803 (2010).
[26] M. Gong, W. Zhang, G.-C. Guo, and L. He, Phys. Rev. Lett. **106**, 227401 (2011).
[27] A. Muller, W. Fang, J. Lawall, and G. S. Solomon, Phys. Rev. Lett. **103**, 217402 (2009).
[28] J. E. Avron, G. Bisker, D. Gershoni, N. H. Lindner, E. A. Meirom, and R. J. Warburton, Phys. Rev. Lett. **100**, 120501 (2008).
[29] R. Trotta, P. Atkinson, J. D. Plumhof, E. Zallo, R. O. Rezaev, S. Kumar, S. Baunack, J. R. Schröter, A. Rastelli, and O. G. Schmidt, Adv. Mater. **24**, 2668 (2012).
[30] S. Kumar, R. Trotta, E. Zallo, J. D. Plumhof, P. Atkinson, A. Rastelli, and O. G. Schmidt, Appl. Phys. Lett. **99**, 161118 (2011).
[31] F. Ding *et al.*, Phys. Rev. Lett. **104**, 067405 (2010).
[32] See Supplemental Material at http://link.aps.org/supplemental/10.1103/PhysRevLett.109.147401 for theoretical and experimental details.
[33] V. Mlinar and A. Zunger, Phys. Rev. B **79**, 115416 (2009).
[34] J. Wang, M. Gong, G. Guo, and L. He, Appl. Phys. Lett. **101**, 063114 (2012).